

Molecular Beacons

Fluorescent Probes for Detection of Endogenous mRNAs in Living Cells

Diana P. Bratu

Summary

A novel approach for detecting nucleic acid in solution has been adopted for real-time imaging of native mRNAs in living cells. This method utilizes hybridization probes, called “molecular beacons,” that generate fluorescent signals only when they are hybridized to a complementary target sequence. Nuclease-resistant molecular beacons are designed to efficiently hybridize to accessible regions within RNAs and then be detected via fluorescence microscopy. The target regions chosen for probe binding are selected using two computer algorithms, *mfold* and *OligoWalk*, that predict the secondary structure of RNAs and help narrow down sequence stretches to which the probes should bind with high affinity in vivo. As an example, molecular beacons were designed against regions of *oskar* mRNA, microinjected into living *Drosophila melanogaster* oocytes and imaged via confocal microscopy.

Key Words: Molecular beacons; fluorescent probes; hybridization; secondary structure prediction; RNA localization; live-cell imaging.

1. Introduction

The direct visualization of specific mRNAs in living cells has been desirable for some time for accelerating the studies of intracellular RNA trafficking and localization, just as green fluorescent protein has stimulated the study of specific proteins in vivo. Tyagi and Kramer have developed a general method using hybridization probes called “molecular beacons,” which generate fluorescence signals as they hybridize to complementary nucleic acid target sequences (*see Fig. 1*) (1). Unbound molecular beacons are nonfluorescent and it is not necessary to remove excess probes to detect the hybrids. These probes bind to their targets spontaneously at physiological temperatures; thus, their introduction into cells is sufficient to illuminate target mRNAs (2–4).

From: *Methods in Molecular Biology*, vol. 319: *Cell Imaging Techniques: Methods and Protocols*
Edited by: D. J. Taatjes and B. T. Mossman © Humana Press Inc., Totowa, NJ

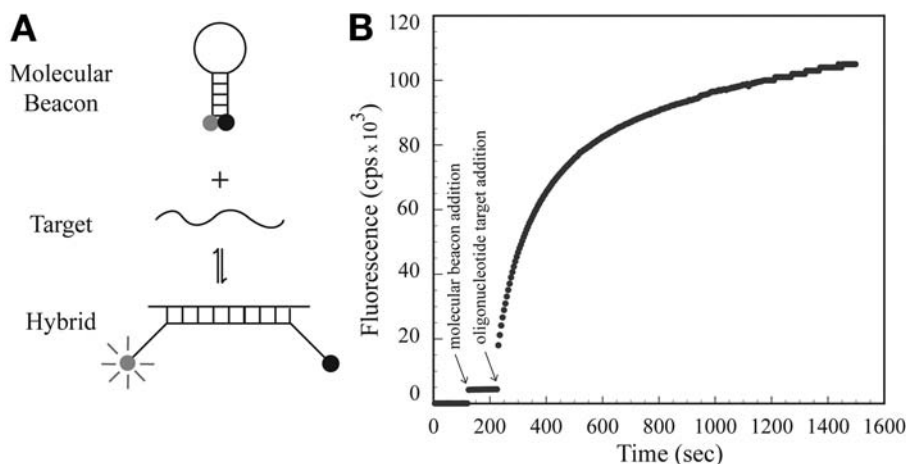


Fig. 1. Principle of operation. Molecular beacons are oligonucleotides that possess complementary sequences on either end of a probe sequence, enabling the molecule to assume a hairpin configuration, in which a fluorophore and a quencher are held in close proximity. When these probes hybridize to a complementary target, the formation of a probe–target hybrid disrupts the hairpin stem, removing the fluorophore from the vicinity of the quencher, and restoring the probe’s fluorescence.

Theoretically, any sequence within a target RNA can be chosen as a site for molecular beacon binding. The endless possibilities give one the confidence that such regions are easily identified. However, the extent of target accessibility is primarily a consequence of complex secondary and tertiary intramolecular structures, which are difficult to predict and can mask many of these regions. Furthermore, inside the cell, mRNAs exist in association with proteins that further occlude parts of the mRNA. Although regions involved in protein binding can only be identified by experimental analysis, reasonable attempts can be made to predict the regions that are not involved in tight secondary structures. So far, several *in vitro* assays and theoretical algorithms are available to help identify putative target sites within mRNA sequences, as well as probes with high affinity for binding (5–8).

The *mfold* RNA-folding algorithm is used to predict the most thermodynamically stable secondary structure along with an ensemble of suboptimal structures (9). Because none of these structures can be considered to represent the naturally occurring conformation, the parameters that describe the entire ensemble are analyzed. The number of candidate sites is winnowed down by employing a second algorithm. OligoWalk scans the folded RNA sequence for regions to which various-length oligonucleotides are capable of binding (10). With consideration of the base composition of each oligonucleotide and of the predicted

secondary structure of the RNA, the output provides information about the stability of the expected hybrid and thus identifies potential target regions.

Once identified, molecular beacons specific for those regions are designed and synthesized. To detect an intracellular target, these probes need to be stable inside the cell and not perturb or destroy its target. Conventional molecular beacons synthesized from deoxyribonucleotides are not suitable for use inside living cells because the single-stranded probe sequence of conventional molecular beacons are subject to digestion by single-strand-specific cellular deoxyribonucleases. Therefore, for *in vivo* studies, molecular beacons are synthesized from unnatural nucleotides possessing an oxymethyl group in place of a hydrogen atom at the 2'-position of their pentose moiety. These modified molecular beacons are resistant to cellular nucleases, and upon binding to RNA, they do not form a substrate for ribonuclease H, thus maintaining the integrity of the target molecule (2).

This chapter describes the steps necessary to find accessible probe-binding target sites within an RNA sequence and to design efficient molecular beacons for RNA detection *in vivo*. The last section provides an example of RNA imaging in living *Drosophila* oocytes.

2. Materials

1. RNAstructure (free download on <http://rna.chem.rochester.edu/index.html> for PC only).
2. Spectrofluorometer (Photon Technology International, South Brunswick, NJ).
3. Spectrofluorometric thermal cycler (Applied Biosystems Prism 7700).
4. Nuclease-free water (Ambion Inc., Austin, TX).
5. TE buffer: 1 mM EDTA, 10 mM Tris-HCl, pH 8.0.
6. 10X Phosphate-buffered saline (PBS) with CaCl_2 and MgCl_2 (Sigma, St. Louis, MO). Dilute to 1X with nuclease-free water or diethyl pyrocarbonate (DEPC)-treated water. Store at room temperature.
7. Molecular beacon. Dissolve stock solutions in nuclease-free water and store at -20°C . Dilute working solutions in 1X PBS, keep protected from light, and store at -20°C for 1 mo.
8. Oligonucleotide target complementary to the probe sequence of the molecular beacon. Dissolve in TE buffer and store at -20°C .
9. *In vitro*-transcribed RNA.
10. Hybridization buffer: 1 mM MgCl_2 , 20 mM Tris-HCl, pH 8.0.

3. Methods

3.1. Selection of RNA Target Regions

3.1.1. Secondary Structure Prediction Using *mfold*

Input the mRNA sequence on the *mfold* RNA server (<http://www.bioinfo.rpi.edu/~zukerm/>) and fold it using the default settings (9). An immediate output is obtained unless the RNA is longer than 800 bp, in which case it is

folded as a “batch.” The completed job is posted within a couple of hours, depending on the server’s availability. The algorithm predicts the most thermodynamically stable secondary structure along with an ensemble of suboptimal structures (the maximum limit can be chosen prior to folding the RNA; a default value of 50 is sufficient for this analysis). Because none of these structures can be considered to represent a naturally occurring conformation, the parameters describing the entire ensemble must be analyzed. The first parameter is ss-count, which defines the probability of a nucleotide to be single-stranded. The second parameter is P-num, a value that denotes the total number of different basepairs that can be formed by a particular base within the set of foldings. These values are assigned to each nucleotide in the mRNA sequence (*see Note 1*).

Once the set of foldings is generated, obtain the following files to be analyzed.

- To view the predicted secondary structure of the RNA, select the jpg option of the first listed structure (the most stable structure in the set).
- To view this folded structure representing the ss-count values, choose the “ss-count” annotation, where each nucleotide (annotated as a dot or character) will be indicated by a color representing the value found in the “ss-count table.” Clicking on the structure image converts this to a color-coded fold (*see Note 2*).
- This window also offers access to the “ss-count table” file. To obtain the actual values, open the file and save it. Open this file in Microsoft Excel; this will provide the opportunity to graph the ss-count value for each nucleotide.
- The P-num values are found in a file accessible from the first output screen. Follow the same steps as for the “ss-count table” to view the secondary structure, save the file, and plot the graph of P-num values for the entire sequence.

3.1.1.1. CRITERIA FOR SELECTING ACCESSIBLE TARGET REGIONS

The ss-count/P-num graph indicates regions of structural plasticity.

- Plot both ss-count and P-mm for each number nucleotide. Adjust ss-count values by x before plotting. The ss-count values are adjusted in order to make them comparable with the range of values for P-num.

$$x = P\text{-mm}_{\max} / (ss\text{-count}_{\max} + 1)$$

$$ss\text{-count}_{\text{adj}} = (ss\text{-count} + 1) \times x$$

- Evaluate the graph and choose regions with the following criteria:
ss-count = high (single-stranded)
P-mm = low (well determined) OR high (poorly determined)

Values for ss-count of more than 50% (probability of being single-stranded) are considered high and are represented by warm colors in the color-annotated secondary structure. Nucleotides involved in double-stranded regions are represented by cool colors. If these regions are well determined,

the P-num values for the nucleotides involved are very low. If a region is flexible, meaning the nucleotides are not found in the same basepair but they form several kinds of basepairs within the predicted structures, then the P-mm is high, representing a poorly determined structure. Such regions are easily determined when evaluating the P-num color-annotated secondary structure (see **Note 3**).

3.1.2. RNAstructure: OligoWalk

The RNAstructure program is a faithful recreation of *mfold* for Windows (10). The OligoWalk program overcomes the need to synthesize a large number of oligonucleotides by using thermodynamic data to find oligonucleotides that bind strongly to a target RNA while offering a fast search interface. Utilizing the most current set of thermodynamic parameters for nucleic acid secondary structure, this algorithm calculates the equilibrium affinity of each set-length complementary oligonucleotide and predicts its overall free energy of binding while taking into account duplex stability, local secondary structure within the target RNA, as well as intermolecular and intramolecular secondary structures formed by the oligonucleotide (10–15).

For each oligonucleotide chosen, the following thermodynamic parameters (ΔG) are calculated in kcal/mol:

$\Delta G_{\text{overall}}$: net ΔG of oligonucleotide–target binding (with consideration of all contributions, including breaking target structure and oligonucleotide–self structure)

ΔG_{duplex} ($\Delta G_{\text{binding}}$): ΔG of the oligonucleotide–target hybrid from unstructured states

$\Delta G_{\text{break target}}$: energy penalty resulting from the breaking of intramolecular target basepairs when the oligonucleotide is bound

$\Delta G_{\text{oligo-self}}$: ΔG of the intramolecular oligonucleotide structure

$\Delta G_{\text{oligo-oligo}}$: ΔG of the intermolecular oligonucleotide structure

Before running the OligoWalk module, several selections must be made. First, a set of optimal and suboptimal structures of the RNA is predicted, using the folding feature of RNAstructure, creating a ‘.ct’ file (connect table) that contains the sequence and basepair information (the sequence must be in caps). Then, the “mode” that determines the types of ΔG calculation for a given sequence is chosen. Use the default mode, “break local structure.” In this mode, the target sequence breaks wherever the oligonucleotide binds ($\Delta G_{\text{break target}}$), oligonucleotides lose pairs in self-structures ($\Delta G_{\text{oligo-oligo}}$ and $\Delta G_{\text{oligo-self}}$) and gain pairs in oligonucleotide–target binding (ΔG_{duplex}). The option to include all suboptimal structures of the target is chosen to determine the total free-energy loss of the target. Each structure’s free-energy loss is weighed according to the free energy of the structure.

Once these options are set, OligoWalk calculations are run for an oligonucleotide concentration of 100 ng/ μ L, ranging in length from 18 to 25 nucleotides. These oligonucleotides are “walked” along the RNA sequence, one nucleotide at a time, until the criteria below are met (*see Note 4*). It is possible for a longer region of the target to be chosen as favorable, not just the region comprising the length of the oligonucleotide. $\Delta G_{\text{oligo-self}}$ and $\Delta G_{\text{oligo-oligo}}$ are disregarded, as the molecular beacon structure is analyzed separately using *mfold* (*see subheading 3.2.1.*).

3.1.2.1. CRITERIA FOR SELECTING TARGET REGIONS

- * $\Delta G_{\text{overall}}$ and ΔG_{duplex} = most negative (–) kcal/mol values;
- * $\Delta G_{\text{duplex}} - \Delta G_{\text{overall}} \leq -10$ kcal/mol;
- * ΔG_{break} = lowest positive (+) kcal/mol values.

3.2. Molecular Beacons

3.2.1. Design

The probe length comprising the hairpin loop can range between 15 and 25 nucleotides. This is dependent on the target region length chosen to be accessible for probe binding. Longer sequence stretches permit probe design flexibility. The %GC composition of the probe sequence should range between 40% and 55%. Two arm sequences designed to be complementary to each other are then added at the respective ends of the probe sequence. Because the rate of hybridization of a molecular beacon is influenced by the stability of its stem, the composition of these sequences is also very important. In practice, the length of the arm sequences is four or five nucleotides and are composed mostly of G/C's (*see Note 5*). Using Zucker's *mfold* folding program, predict the structure of the molecular beacon. The sequence should not form unwanted secondary structures (*see Note 6*).

3.2.2. Signal-to-Background Ratios

Signal-to-background ratio measurements indicate the purity of a molecular beacon preparation. Because of the presence of oligonucleotides that possess only a fluorophore and not a quencher, or of inefficient quenching between the two moieties, the fluorescence signal resulting from the presence of the target is obscured by background fluorescence, leading to inaccurate hybridization measurements (*16*). The fluorescence of the molecular beacon in a 150- μ L solution of 1 mM MgCl_2 , 20 mM Tris-HCl, pH 8.0 is determined (F_{buffer}) using the optimal excitation and emission wavelength of the fluorophore. After 10 μ L of a 0.1 μ M molecular beacon solution is added, a new fluorescence level is recorded (F_{closed}). The increase in fluorescence is monitored

after a fivefold molar excess of a complementary oligonucleotide is added to the solution. F_{open} is the maximum level of fluorescence reached after the reaction is complete.

The signal-to-background ratio equals $(F_{\text{open}} - F_{\text{buffer}})/(F_{\text{closed}} - F_{\text{buffer}})$. Good molecular beacons generate a fluorescent signal at least 30 times more intense than in the absence of target.

3.2.3. Determination of Thermal Denaturation Profiles

The design of molecular beacons is highly permissive. They can be designed so that they are stable and function under a broad set of conditions. Combinations of loop and stem lengths can be chosen to detect various nucleic acid targets (see Fig. 2).

The fluorescence of molecular beacon solutions should be measured over a wide range of temperatures. Equimolar molecular beacon solutions are prepared in the hybridization buffer. Add a fivefold molar excess of an oligonucleotide that is perfectly complementary to the molecular beacon's probe sequence. In a spectrofluorometric thermal cycler, decrease the temperature from 95°C to 25°C in increments of 1°C. To ensure that equilibrium is reached at each temperature step, the steps should last at least 30 s.

The melting profiles of the probes alone and of their hybrids should indicate correct molecular beacon characteristics (see Fig. 2).

3.2.4. Testing Putative Probes: In Vitro Hybridization to RNA

Prior to using molecular beacons in living cells, in vitro-transcribed full-length RNA is used as a target molecule for in vitro hybridization reactions to determine whether the molecular beacons that were predicted to work well by the computer programs were in fact able to bind to their intended target sequences. The intensity of the fluorescence signal and the rate of hybridization are measured in a spectrofluorometer. These reactions are performed with "naked" RNA under plausible physiological conditions and are not carried out in the presence of a cellular extract that contains the various factors that might have an affinity for the mRNA. Each molecular beacon should be tested for its ability to hybridize to the mRNA in vitro. Even though each molecular beacon could bind spontaneously to an oligonucleotide that is complementary to its probe sequence, only a few might bind efficiently to full-length transcripts.

1. Prepare full-length RNA by in vitro transcription.
2. Measure the fluorescence intensity of a 125-μL solution containing 1 mM MgCl₂, 20 mM Tris-HCl, pH 8.0, and 80 nM of molecular beacon at 25°C until no change in fluorescence occurs.

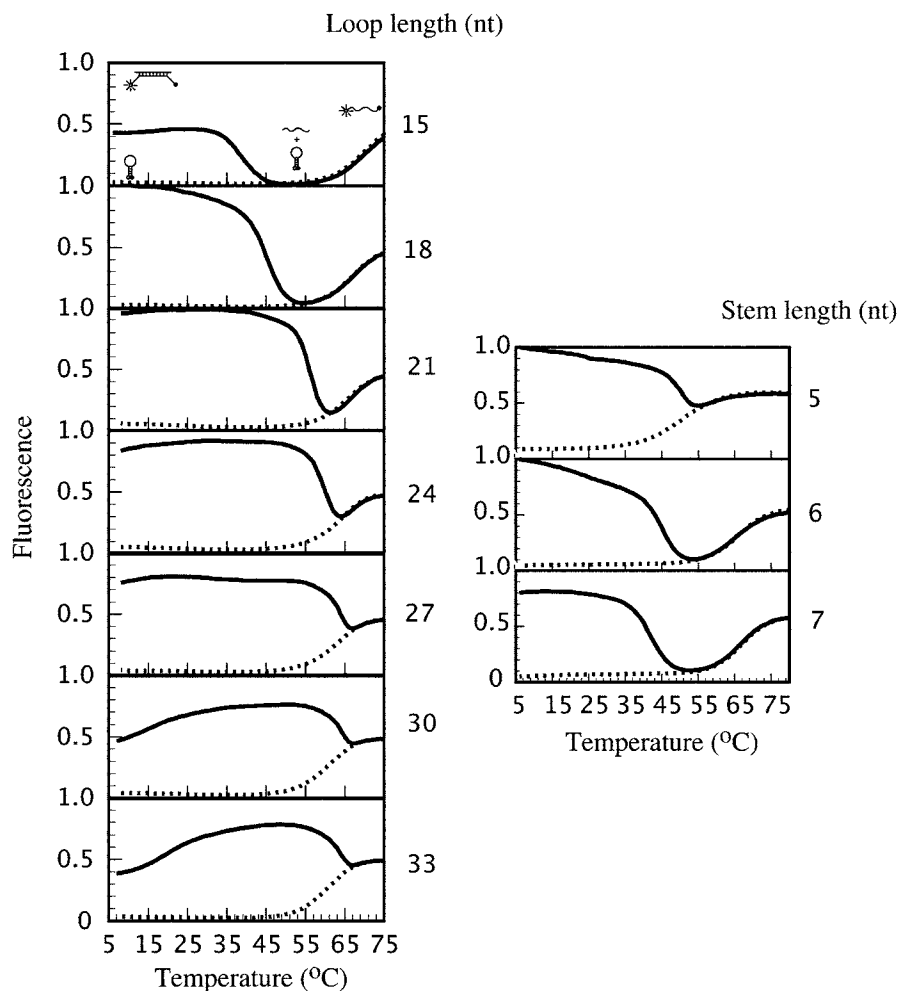


Fig. 2. Thermal denaturation profiles of DNA molecular beacons, alone (dotted lines) or bound to target (continuous lines), where fluorescence intensity was measured as a function of temperature. **(A)** The loop length of a molecular beacon, comprising the probe sequence, was increased in increments of three nucleotides at a time while maintaining a constant stem length of six nucleotides. The melting transition of the probe–target hybrids shifted toward higher temperatures, indicating an increase in the stability of the hybrids. **(B)** The stem length was increased 1 nucleotide at a time while maintaining a constant loop length of 15 nucleotides. The melting transition of the probe–target hybrids shifted toward lower temperatures, indicating a destabilization of the probe–target hybrids, while the melting transition of the molecular beacon stem shifted toward higher temperatures.

3. Add a 5- μ L aliquot of 100 nM transcribed mRNA to this solution and measure the subsequent change in fluorescence as a function of time at 25°C (see **Note 7**). The time-course of hybridization is recorded at the optimal excitation and emission wavelengths of the fluorophore coupled to the molecular beacon (see **Note 8**).

3.3. In Vivo Detection of Oskar mRNA

The mRNA sequence encoded by the *Drosophila melanogaster* maternal gene *oskar* is shown as a model target for in vivo detection with molecular beacons. *Oskar* mRNA localizes during mid-oogenesis in a tight sliver at the posterior pole of the oocyte. Utilizing the RNA secondary structure prediction program *mfold* and applying the aforementioned criteria for selection of accessible target regions, sequences within the mRNA were identified. These regions are either single-stranded or paired with distant sequences in most of the thermodynamically favorable foldings and contained both flexible and stable structures.

Next, using OligoWalk's thermodynamic outputs, which reflected the degree of stability of all RNA-probe hybrids formed from scanning oligonucleotides, the choice of target sequences was narrowed down to 11 regions (see **Fig. 3**). Among the 11 regions selected for *oskar* mRNA, 4 regions (*osk* 62–87, *osk* 964, *osk* 2209, and *osk* 2579) had high values for both ss-count and P-num. The threshold value for the selection of these regions was 220, which represents a 50% probability that the respective region is single-stranded and is a measure of how “well determined” the structure formed by the sequence is. The remaining seven regions had low P-num values, indicating better determined and more stable regions. This theoretical analysis helped reduce the number of potentially accessible target regions and, with good confidence, provided sequences for *oskar* mRNA-specific molecular beacons.

A 100 ng/ μ L-solution of the *oskar* mRNA-specific molecular beacon dissolved in nuclease free water was microinjected into a stage 9 *Drosophila melanogaster* oocyte (see **Fig. 4**) (17). The images acquired at various time intervals revealed a homogenous distribution of the molecular beacons with an increased fluorescent signal at the posterior end of the oocyte (see **Note 9**) (2).

4. Notes

1. *mfold* values:

- ss-count is the number of times that the *i*th base is single-stranded in *n* predicted foldings.
- P-num (*i*) = $\sum_{k < i} \phi (\Delta G(k,i) \leq \Delta G + \Delta \Delta G) + \sum_{i < j} \phi (\Delta G(i,j) \leq \Delta G + \Delta \Delta G)$, where *i*, *j*, and *k* are bases and ϕ is defined as 1 when expression is true and 0 otherwise.

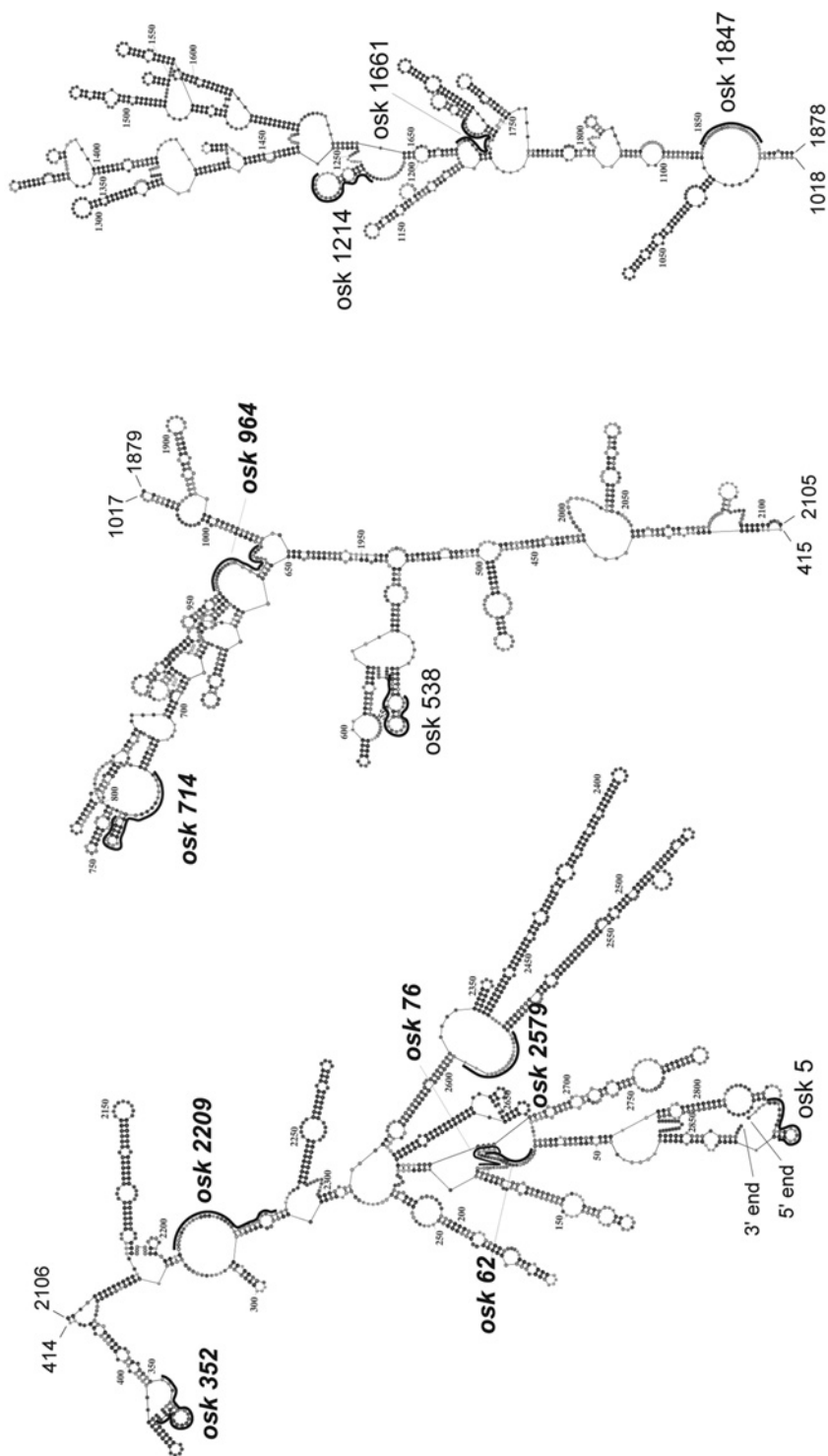


Fig. 3. Most stable secondary structure of *oskar* mRNA showing the location of molecular beacon target sequences. The computer-folded structure is depicted in three segments, with the connecting nucleotides indicated at the break points. The bold nomenclatures represent regions that were most accessible by the molecular beacons.

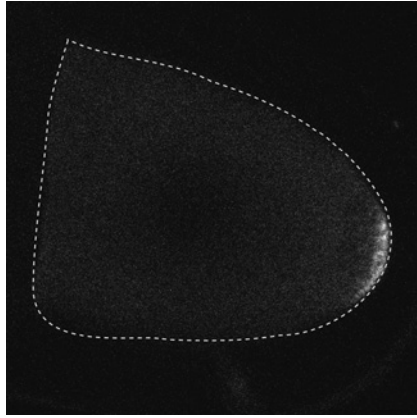


Fig. 4. Stage 9 *Drosophila* oocyte injected with a molecular beacon solution specific for *oskar* mRNA. After 10 min, an image was acquired using a confocal microscope. Anterior is to the left and posterior is to the right of the image.

- ΔG is the overall minimum free-energy of any folding that contains the i,j basepair:

$$\Delta G = \min_{1 \leq i < j \leq n} \Delta G(i,j).$$

- $\Delta\Delta G$ is a user-selected free-energy increment set at $1 \leq \Delta\Delta G \leq 12$ (kcal/mol)

$$\Delta\Delta G = \Delta G \times P/100.$$

- P is the parameter that controls the value of the free-energy increment $\Delta\Delta G$. The default value is 5.
2. To save this structure as a “.pdf” file, choose the output option as a “postscript” file. Click on the structure and the option to “save as” is available in a pop-up window. Save this as a “.cgi” file, which can then be converted to a “.pdf” file with Acrobat Distiller. View and manipulate in Adobe Illustrator.
 3. Unlike predictions of local hairpins, long-range interactions or multibranch junctions remain poorly determined. Such predicted structures could provide insights into regions of potential structural plasticity within an RNA molecule and thus reveal potential accessible sites for antisense probes. Therefore, when considering probes for targeting an RNA sequence, it is very helpful to pay close attention to the information offered by a secondary structure fold.
 4. In vivo, the mRNA structure is dependent on the intracellular environment. For example, mRNA accessibility becomes less predictable, as the structures of actively translated mRNAs are transiently altered by passing ribosomes. Also, the stability of the duplexes formed by probes and complementary nucleic acids is influenced by the presence of RNA-binding proteins. These might mask target

sites, preventing hybridization from occurring. Therefore, a number of different regions distributed throughout the mRNA sequences should be considered as target sites for molecular beacons.

5. Because the 2'-*O*-methyl backbone renders molecular beacons capable of forming stronger stems, the sequence composition of the complementary arms are either four nucleotides for shorter-length probe sequences or five nucleotides for longer hairpin loops. For example, molecular beacons with 15–18 nucleotides composing the hairpin loops should have stems such as CGGC (or a variation of this order). For longer loops, design stems such as GATCC or GGAGC. A 100% GC five- nucleotide stem is too strong and the molecular beacon would not open at room temperature under cellular conditions.
6. The structures generated by the folding program should have the intended hairpin structure. Any other structure that does not form the set-length stem hybrid will generate inefficient binding probes (i.e., the stem is longer, or the nucleotides within the hairpin loop form basepairs) or high-background signals (when the nucleotides at the 5' and 3' ends of the sequence do not form a pair, the fluorophore is removed from the vicinity of the quencher). In either instance, both the probe and stem sequences can be manipulated. If the chosen region on the RNA permits, shift the frame of the probe along the target sequence until a probe structure with minimal self-complementarity is obtained. For a longer hairpin loop, a small interior stem of two to three nucleotides long does not significantly affect the performance of a molecular beacon. If the alternative structures arise from the choice of the stem sequence, change its composition to ensure a hairpin conformation. The stem can also be formed by terminal nucleosides of the probe sequence.
7. For each molecular beacon tested, the kinetic characteristics of hybridization as well as the level of fluorescence generated might be different. The most accessible target sequences induce the fastest increase in fluorescence. However, the efficiency of hybridization and stability of binding can depend on more than the secondary structure of the RNA. The probe's size and sequence composition are important determinants of the stability of the resulting hybrid. For *oskar* mRNA, each probe has approx 40% GC composition and is 18 to 25 nucleotides in length. The rate of binding might also be influenced by the tertiary structure of the RNA. The sites accessible for targeting could be masked by the three-dimensional folding of the molecule or by other tertiary interactions, such as prestacking of the single-stranded regions. For these reactions, the molecular beacon molar concentration exceeds that of the target RNA to ensure that all RNA molecules are bound by a probe.
8. Molecular beacons can be labeled with a wide range of fluorophores, which can be efficiently quenched by the same quencher, such as dabcyI, BHQ1, or BHQ2 (16,18). A list of companies licensed to synthesize molecular beacons as well as a list of the available fluorescent labels can be found at <http://www.molecular-beacons.org/>.
9. When images are acquired by a confocal fluorescence microscope, the background signal from other focal planes generated by the nonspecific binding of cellular components to probes that changes their conformation and causes them to fluoresce is

eliminated. When conventional fluorescence microscopy is implemented, the images can be enhanced via deconvolution analysis, where the fluorescence contribution from other focal planes is removed, or by ratio imaging, where the intensity of the fluorescence generated by the specific molecular beacon is divided by the intensity of the spectrally distinguishable fluorescence of a second, nonspecific molecular beacon that is coinjected in an equimolar cocktail with the specific molecular beacon.

Acknowledgments

The author thanks Sanjay Tyagi and Fred Russell Kramer for their assistance and advice and Salvatore A.E. Marras for help with molecular beacon synthesis. This work was supported by National Institutes of Health grants ES-10536 and EB-00277.

References

1. Tyagi, S. and Kramer, F. R. (1996) Molecular beacons: probes that fluoresce upon hybridization. *Nature Biotechnol.* **14**, 303–308.
2. Bratu, D. P., Cha, B. J., Mhlanga, M. M., Kramer, F. R., and Tyagi, S. (2003) Visualizing the distribution and transport of mRNAs in living cells. *Proc. Natl. Acad. Sci. USA* **100**, 13,308–13,313.
3. Matsuo, T. (1998) In situ visualization of messenger RNA for basic fibroblast growth factor in living cells. *Biochem. Biophys. Acta* **1379**, 178–184.
4. Sokol, D. L., Zhang, X., Lu, P., and Gewirtz, A. M. (1998) Real time detection of DNA:RNA hybridization in living cells. *Proc. Natl. Acad. Sci. USA* **95**, 11,538–11,543.
5. Southern, E. M., Milner, N., and Mir, K. U. (1997) Discovering antisense reagents by hybridization of RNA to oligonucleotide arrays. *Ciba Found. Symp.* **209**, 38–44; discussion 44–46.
6. Ho, S. P., Bao, Y., Leshner, T., et al. (1998) Mapping of RNA accessible sites for antisense experiments with oligonucleotide libraries. *Nature Biotechnol.* **16**, 59–63.
7. Lima, W. F., Mohan, V., and Crooke, S. T. (1997) The influence of antisense oligonucleotide-induced RNA structure on *Escherichia coli* RNase H1 activity. *J. Biol. Chem.* **272**, 18,191–18,199.
8. Milner, N., Mir, K. U., and Southern, E. M. (1997) Selecting effective antisense reagents on combinatorial oligonucleotide arrays. *Nature Biotechnol.* **15**, 537–541.
9. Zuker, M. (2003) Mfold web server for nucleic acid folding and hybridization prediction. *Nucleic Acids Res.* **31**, 1–10.
10. Mathews, D. H., Burkard, M. E., Freier, S. M., Wyatt, J. R., and Turner, D. H. (1999) Predicting oligonucleotide affinity to nucleic acid targets. *RNA* **5**, 1458–1469.
11. Peyret, N., Seneviratne, P. A., Allawi, H. T., and SantaLucia, J., Jr. (1999) Nearest-neighbor thermodynamics and NMR of DNA sequences with internal A.A, C.C, G.G, and T.T mismatches. *Biochemistry* **38**, 3468–3477.

12. SantaLucia, J., Jr. (1998) A unified view of polymer, dumbbell, and oligonucleotide DNA nearest-neighbor thermodynamics. *Proc. Natl. Acad. Sci. USA* **95**, 1460–1465.
13. SantaLucia, J., Jr., Allawi, H. T., and Seneviratne, P. A. (1996) Improved nearest-neighbor parameters for predicting DNA duplex stability. *Biochemistry* **35**, 3555–3562.
14. Sugimoto, N., Nakano, S., Katoh, M., et al. (1995) Thermodynamic parameters to predict stability of RNA/DNA hybrid duplexes. *Biochemistry* **34**, 11,211–11,216.
15. Xia, T., SantaLucia, J., Jr., Burkard, M. E., et al. (1998) Thermodynamic parameters for an expanded nearest-neighbor model for formation of RNA duplexes with Watson-Crick base pairs. *Biochemistry* **37**, 14,719–14,735.
16. Marras, S. A., Kramer, F. R., and Tyagi, S. (2002) Efficiencies of fluorescence resonance energy transfer and contact-mediated quenching in oligonucleotide probes. *Nucleic Acids Res.* **30**, e122.
17. Bratu, D. P. (2003) *Imaging Native mRNAs in Living Drosophila Oocytes Using Molecular Beacons*. New York University, UMI Dissertation Service, New York, New York.
18. Tyagi, S., Bratu, D. P., and Kramer, F. R. (1998) Multicolor molecular beacons for allele discrimination. *Nature Biotechnol.* **16**, 49–53.